

PROCEDURE OF GROUND VIBRATION EXPERIMENTS ON AIRCRAFT WITH SIMULATING FORCES DUE TO ENGINE IMBALANCE AT BLADE LOSS

Regina V. Leonteva
PSC "Tupolev"

Keywords: *engine imbalance, simulation, ground vibration tests*

Abstract

Simulation of inertial forces from the engine with imbalance at blade loss during ground vibration tests (GVT) is considered. Airplane forced oscillations in case of the non-rotating engine rotor are measured.

Experimental procedure with measurements in frequency domain and time domain, implementation of rotating forces, assessment of capability for superposition of oscillations are presented.

Some results obtained due to the engine imbalance simulation on the transport airplanes with two or four engines on pylons under the wing are given.

1 Introduction

For safety assessment of the airplane flight with the engine imbalance due to blade loss it is necessary to obtain the calculated and the experimental data.

The purpose of experiments with the imbalance simulation is the measurement of accelerations in different points on the airplane and the refinement of preliminary calculations of loads at engine's blade loss in flight.

Generally, it is referred to the linear structural model of the airplane, excluding non-linearity effects, actual damping characteristics and other design features.

During experiments there is the influence of all modes of the symmetric and the antisymmetric spectra with their non-linear

dependence of elastic forces and damping forces on the oscillation amplitude.

2 Force Actions at Imbalance

Airplane oscillation equations during GVT with simulating forces at engine's blade loss can be represented as:

$$C \ddot{q} + H \dot{q} + G q = Y_F^T F^I + Y_M^T M^G, \quad (1)$$

where q - generalized coordinates vector, $q_1, \dots, q_m, \dots, q_n$; C , H and G - inertia matrix, structural damping matrix and structural stiffness matrix, respectively. The right side of the equation - external forces - is represented by a vector of inertial forces F^I from engine imbalance and a vector of gyroscopic moments M^G arising from engine's angular vibration. Y_F^T , Y_M^T - transposed transition matrices from the forces and the moments in the "physical" coordinates y to the generalized coordinates q .

Caused by blade loss the vector of inertial force, rotating in the plane normal to the engine rotor axis, is written as:

$$F^I = [0, \dots, f_m, \dots, 0]^T, \quad (2)$$

$$f_m = \omega^2 (rm),$$

where ω - rotational speed of engine rotor, m - a missing rotor mass, r - the radius from the rotor axis to the center of gravity of m , f_m - the resultant force of all blades in damaged section of the engine.

Projections of rotating vector of inertial force on the vertical axis y and the lateral axis z , are equal to

$$F_y = \omega^2 (rm) \cos(\omega t), \quad (3)$$

$$F_z = \omega^2 (rm) \cos(\omega t + \pi / 2).$$

Gyroscopic moment is proportional to the rotor axial moment of inertia I_x and the vector product of ω and the rate of engine's angular oscillations Ω , (Fig. 1):

$$M^G = I_x [\omega \times \Omega]. \quad (4)$$

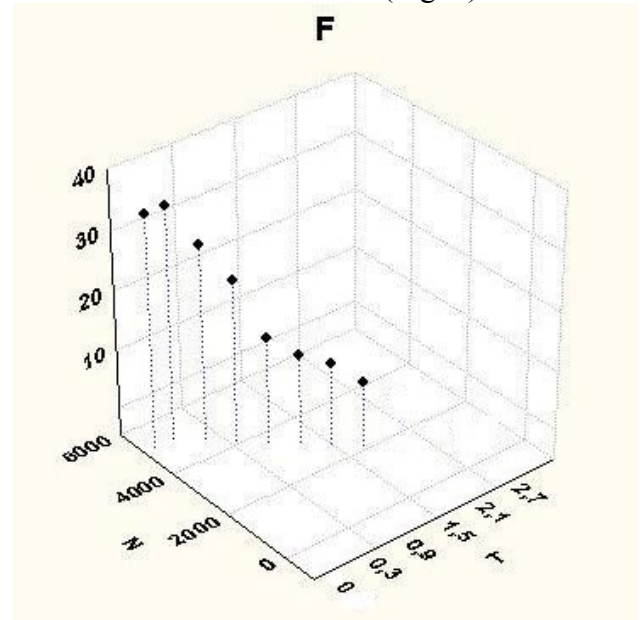


Fig 1. Force actions in vibrations of rotating engine with a lost blade

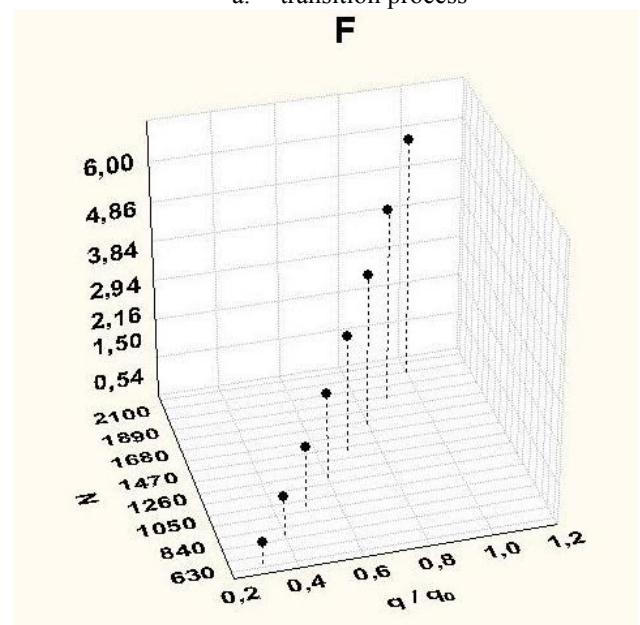
Transition process is described by the same equation (1), in the right side it (instead of depending of the inertial force and the gyroscopic moment on specified value of frequency ω) occurs dependence on the derivative of angular displacement θ of the rotor with respect to time: $\omega = \dot{\theta}$.

3 Features of Modeling Processes in Time Domain and Frequency Domain

After engine's blade loss and in-flight engine shutdown there are two main stages in time: transition process (from cruising rpm to stationary) and steady – windmilling, with constant rpm, which is determined by the current value of dynamic pressure, Mach number M and altitude H (Fig. 2).



a. transition process



b. windmilling

Fig. 2. Dependence of inertial force on time t , rpm N , and dynamic pressure

Therefore, the force simulation problem at imbalance is split into two. The first is to simulate transient processes with continuous variation of frequency and amplitude of the excitation forces in real time scale, the second is

to simulate steady oscillations for each value of dynamic pressure.

Measuring the frequency characteristics should be conducted on the maximum allowable levels of excitation (the lowest interference effect), but these measuring should be repeated at lower levels to assess the effect of nonlinearity of the structure.

In this case we obtain the experimental data on the effect of nonlinearity on the values of accelerations at specified points. The maximum accelerations are determined by their values obtained in the process of determining natural frequencies and mode shapes associated with the engine oscillations.

Experiments with the engine imbalance simulation are performed during the "regular" GVT of the airplane, in order to minimize the number of equipment permutations and reduce the overall time. It is important that the duration of the considered measurements is minimal, not exceed a half of the work shift in testing.

4 Implementation of rotating forces

To generate the resultant rotating force it is enough to apply two of its projection - fixed - to the engine, in one of its sections, assuming that the rotor axis is undeformable. In this case, the change of the selected section requires moving the force application points.

It is required two resultant forces F_1, F_2 to generate the gyroscopic moment, thus - a doubling of resources due to the second couple of fixed forces (Fig. 3).

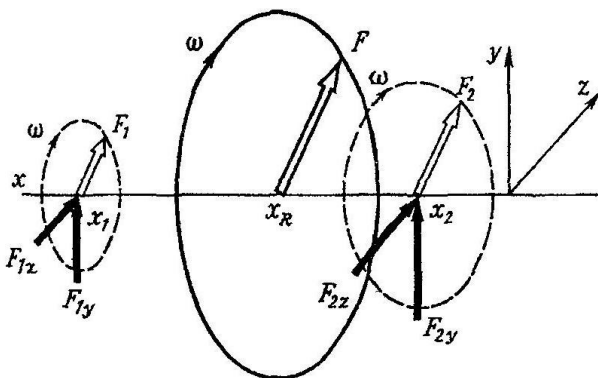


Fig. 3. Inertial force simulation on the non-rotating engine: F_1, F_2 - resultants of a couple of fixed forces, F - rotating resultant forces

The advantage of this option is the ability to move the resultant inertial force along the engine axis without any permutations, and the lack is essential complication of the experiment.

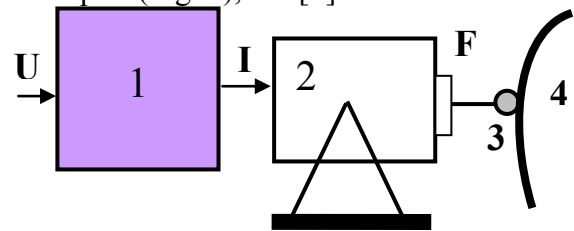
It is decided to limit the simulation only the rotating inertial force in one of engine's sections, leaving the evaluation of the effect of the gyroscopic moment for calculations, see [1].

The simplest version of modeling the inertial force (at imbalance) is associated with the use of two fixed-mounted electrodynamic exciters, controlled by sine generator signals with phase shifted by 90 degrees.

The combination of this exciter with a special - modal - power amplifier converts the control input voltage U into a proportional mechanical force F applied to the moving system of exciter

$$F = EU, U = \frac{\omega^2 rm}{E}, \quad (5)$$

where E - gauge coefficient of amplifier-exciter pair (Fig. 4), see [2].



1- power amplifier, 2- exciter, 3- force sensor, 4- engine
Fig. 4. Vibration excitation (simplified) scheme

5 Superposition of unidirectional forces - experimental estimation

In the case of the (engine) linear structure provided non-deformable rigid body, the rotating force can be replaced by superposition of two projections of force on its axis y, z . If the structure characteristics are retained, then it possible to sum the engine vibrations caused by each of these projections, applied at different times (Fig. 5). However, for the non-linear system the superposition principle does not apply, by definition.

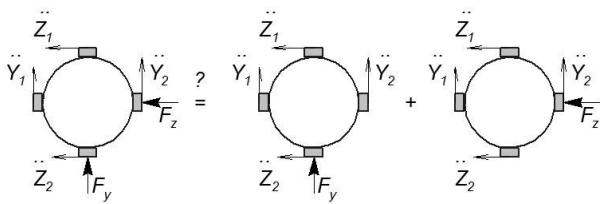


Fig. 5. Verifying the superposition of oscillations under action of sequential excitation

The assessment of the admissibility of the superposition of oscillations caused by alternately excited by vertical or horizontal forces for a particular engine presents the practical interest. Because of the nonlinearity of characteristics on the real airplane, the vector summation of these oscillations at different frequencies differ from the vibrations caused by the rotating force, but the quantitative aspect of these differences is very important. In the case of positive result it could be adjusted the calculation according to experimental data with sequential measurements of steady oscillations caused by vertical harmonic force of excitation or lateral one.

In [3] it was shown data obtained with the simulation of rotating forces during GVT on A340-500 aircraft with two engines mounted on pylons. That data were obtained for almost steady, forced oscillations (windmilling) with a continuous change of the excitation frequency $\omega(t)$ in the range of 9-50 Hz, and 1-12,5 Hz

6 Experimental data results

Examples are presented by data obtained during regular GVT on transport airplanes: with 2 and 4 engines, further identified as No.1 and No.2.

Vibration excitation was realized by Prodera electrodynamic exciters, data collection and excitation control – by LMS equipment. On engines at each excitation point there were force sensors and accelerometers, mounted in pairs at vertical and lateral directions.

In the range of frequencies associated with engine oscillations, the accelerations were measured by signals of all accelerometers during excitation of vibrations of one of the engines simultaneously in vertical and lateral directions, and, alternately, (separately), in each of them.

Fig. 6 shows the survey of experimental frequency characteristics of engine accelerations for two airplanes. Resonant frequencies of the first engine modes were 2.5 and 3.9 Hz for airplane No.1, 2.2 and 4.7 Hz - for airplane No. 2.

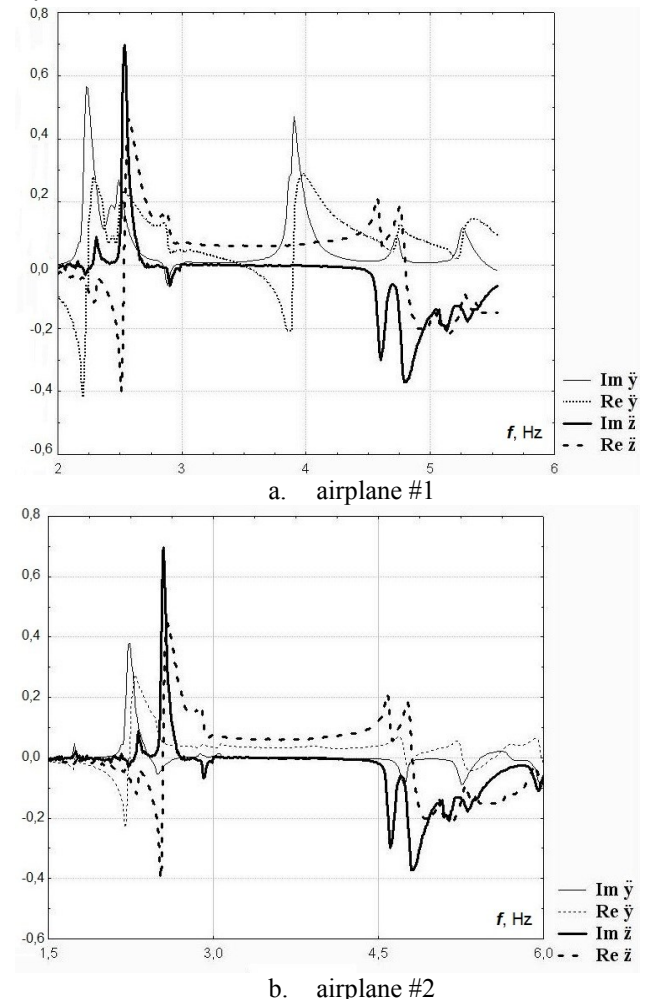


Fig. 6. Experimental resonance curves for engine accelerations

In the process of modeling imbalance the systematic errors could occur on airplanes. Such error, in particular, was caused by the difference of the amplitudes of vertical and horizontal excitation forces (even in the absence of the engine oscillations). Their inequality led to a difference in locus of the resultant force from the circle, it was an ellipse. Major axis was directed along the force with the highest amplitude, small - along the other force.

In the tests for technical reasons the specified levels of vertical and lateral excitations (voltage to the power amplifier input recalculated in force) were differed by 50%. Difference of acceleration amplitudes at

frequencies close to resonances engines were amounted up to 10% for the vertical oscillations and up to 15% for horizontal oscillations. Therefore, resultant rotating force applied to the engine, were respectively changed in amplitude, and the locus of this force vector were described as ellipse (in the plane normal to the axis of the engine).

In Fig. 7 it is shown the amplitude-frequency (AFC) and phase-frequency (PFC) characteristics of the forces at the excitation points of engines (airplane No. 1) from signals of force sensors.

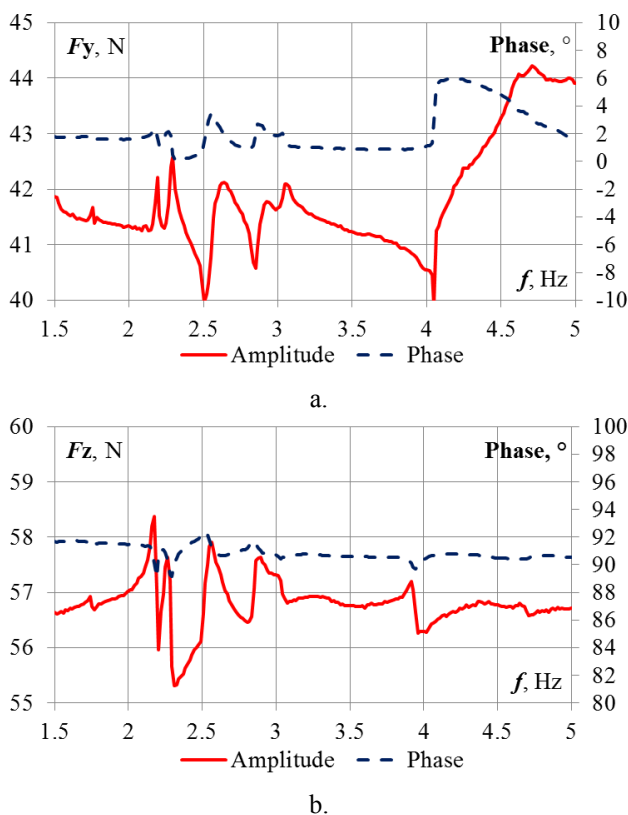


Fig. 7. Amplitude-frequency and phase-frequency characteristics of the forces along two axes F_y and F_z at the engine excitation points

Differences between the vector sums of the forces at excitations points of the engine and at points where the forces applied to the exciter moving system are maximal in the vicinity of the resonance frequencies, where there are the highest amplitudes. In particular, for airplane No.1 the greatest changes are amounted up to 11% at a higher frequency and up to 6% at lower frequency.

Fig. 8 shows the ratio of the vertical and the lateral force modules from force sensors.

The quaint frequency locus of force amplitudes was generated with changing frequency. In the case of constant amplitudes, this frequency locus should be contracted to the point all frequencies. Obviously, the frequency locus for the resultant rotating force is also distorted (is not shown on figure).

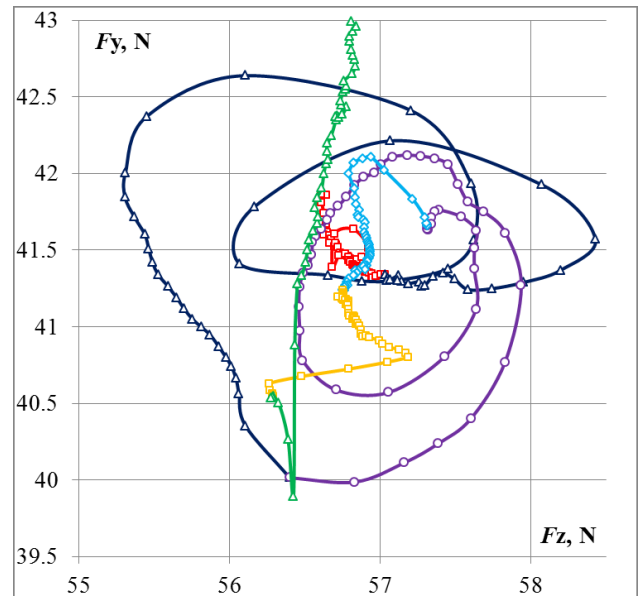


Fig. 8. Change in the ratio of amplitudes of forces with increasing frequency

The difference between the engine's forced oscillations of airplane No.1, obtained in simulation of the rotating inertial force and the superposition of oscillations, caused only by one vertical force or one lateral force, sequentially, can be seen on the frequency response (Fig. 9).

Comparison of accelerations at the engine checkpoint shows the essential difference, primarily, near the extrema at the resonance frequencies. The major causes for the violation of the superposition principle of oscillations are nonlinearities in the stiffness characteristics and in the damping properties of the airplane structure. At the same time, the superposition of oscillations within the linear analysis, given in [3], was quite successful.

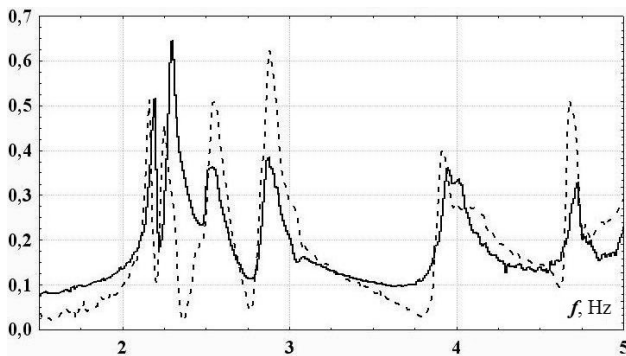


Fig. 9. Amplitude-frequency characteristics of the accelerations at the engine excitation point for rotating force F - dotted line and at superposition of forces F_y and F_z - solid line

7 Conclusion

GVT on the airplane with imbalance simulation are used for the refinement of load calculations at engine's blade loss in flight. Power impacts during forced oscillations of the damaged engine include the inertial force and the gyroscopic moment. In order to reduce the labor intensity and the testing time it is evident to perform simulation of inertial force only.

Experimental verification of the acceptability for the superposition of vibrations caused, sequentially, by unidirectional excitation forces instead of a couple forming the rotating force, show the essential difference in results of such replacements.

Simulating the engine imbalance on transport airplanes with 2 and 4 engines confirms the possibility of correct modeling of forces during GVT.

The author would like to thank her colleagues: O.A Kuznetsov, M.A. Pronin, V.V. Ferapontov, V.I. Smyslov and I.G. Stepanenko for their support and assistance.

References

- [1] Kuznetsov O.A, Leontieva R.V. Dynamic loads on aircraft due to engine imbalance at blade off. Report S5B. *International Forum on Aeroelasticity and Structural Dynamics*, June 24-26, 2013. Bristol, Great Britain.
- [2] Kuznetsov O.A, Smyslov V.S. *Engine imbalance at blade off and the forced vibrations of the aircraft - calculation and experiment*. Trudy TsAGI, Issue 2714. TsAGI Publishers, 2013. Moscow, Russia.
- [3] Lubrina P. Ground vibration experiments on large civil aircraft for engine imbalance purpose.

International Forum on Aeroelasticity and Structural Dynamics, June 24-27, 2003. Stockholm, Sweden.

Contact Author Email Address

Mailto: regina.leontjeva@gmail.com

Copyright Statement

The authors confirm that they, and/or their company or organization, hold copyright on all of the original material included in this paper. The authors also confirm that they have obtained permission, from the copyright holder of any third party material included in this paper, to publish it as part of their paper. The authors confirm that they give permission, or have obtained permission from the copyright holder of this paper, for the publication and distribution of this paper as part of the ICAS 2014 proceedings or as individual off-prints from the proceedings.